The Effect of siRNA-mediated Shank3 knockdown on Immunocytochemistry Staining and Motility in Dorsal Root Ganglia Growth Cones

Rebecca Healey

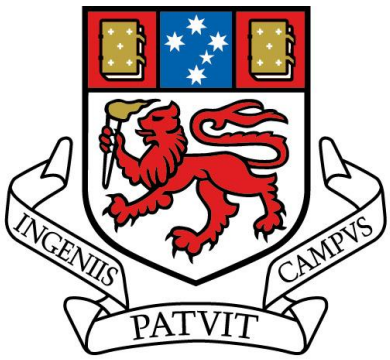

UNIVERSITY OF TASMANIA

A report submitted as a partial requirement for the degree of Bachelor of Psychological Science with Honours at the University of Tasmania, 2019

Statement of Sources

I declare that this report is my own original work and that contributions of others have been duly acknowledged.

Signed: Rebecca Healey, 04/11/19.

Acknowledgements

I hope that in five years' time, when my thesis is collecting dust on a bookshelf in the Psychology Test Library, I will have the opportunity to come back, open that little fabric book, and look fondly on my Honours year. Because despite the difficulty of this year, if there is anything I should feel, it is fondness and appreciation for the people who supported me.

Firstly, I would like to thank my supervisors, Drs Robert Gasperini and Michael Garry for their guidance throughout this period, and their empathy, insight, and patience.

Secondly, I would like to thank Daniel Bligh and Silvia Vicenzi for giving up their time to help me learn some very technically demanding dissection, cell culture, live cell imaging, and immunocytochemistry techniques. If could meet the scientist that I was eight months ago, I would want to push her in a bin, so I can only imagine how they must have felt trying to train me.

Thirdly, I would like to thank Dr Lisa Foa, Dr Katherine Southam, Hayden Arnott, and Taylah Leader for welcoming me into their lab group, and making me feel like part of the medical research community.

I also would like to acknowledge the people (and one Labrador) who actually had to live with me, deal with me, or socialise with me on a day to day basis, and who witnessed firsthand my gradual decline into a hideous, dishevelled, emotional goblin creature: Mum, Jove, Christina, Cashew and my friends in the 2019 Psych Honours cohort.

And finally, I'd like to thank myself for getting help when I needed it, for not giving up and switching projects when it was too hard, and for sticking out the year.

Table of Contents

List of Tables and Figures

The Effect of siRNA-mediated Shank3 knockdown on Immunocytochemistry Staining and Motility in Dorsal Root Ganglia Growth Cones

Rebecca Healey

Word Count: 9805

Abstract

Mutations of the Shank3 gene have consistently been identified as a risk factor for Autism Spectrum Disorder, and are associated with neurological abnormalities indicative of neural connectivity issues. This project aimed to elucidate the functions of Shank3 protein in the growth cone during neural development. It was hypothesised that in dorsal root ganglia growth cones, Shank would colocalise with Homer1b/c (a protein that regulates intracellular calcium responses to BDNF), that siRNA-mediated knockdown of Shank3 protein would reduce Shank expression, and that Shank3 knockdown would abolish growth cone turning responses to BDNF. Shank and Homer appeared to colocalise in the growth cone. However, Shank3 knockdown did not decrease protein expression, and cell culture issues required that turning assays be terminated. As such, this research infers a role of Shank protein in peripheral nervous development but is unable to clarify the specific implications of this for axon pathfinding. Directions for future research include addressing cell culture issues, and repeating knockdown and turning experiments on hippocampal cells known to express Shank3 in the growth cone.

Neurodevelopmental and Autism Spectrum Disorders

Neurologically diverse individuals experience differences in social behaviour, physical development, and cognitive processing, that are atypical of ordinary development, and often associated with functional impairment. For instance, the Diagnostic and Statistical Manual of Mental Disorders (DSM-V) (American Psychological Association, 2013) characterises Autism Spectrum Disorder (ASD) as a neurodevelopmental disorder, with diagnostic features including abnormalities during socialisation, and engagement in atypical and often ritualistic behaviour. Diagnoses encompasses wide variation in phenotypes and functional impairments (American Psychological Association, 2013), and are often comorbid with intellectual disability (ID) (Kaufman, Ayub & Vincent, 2010). Following a meta-analysis of European, Australasian, American and African pervasive developmental disorder (PDD) studies, Elsabbagh et al. (2012) estimated a global PDD prevalence rate of 62 per 10 000 people, and 17 per 10 000 people for ASD.

As diagnosis is lifespan persistent (American Psychological Association, 2013), adults with ASD often experience poor psychosocial outcomes. Howlin, Goode, Hutton and Rutter (2004) report reliance on unsatisfying or menial jobs and lack of independence (such reliance on family members for care, or need for supported living) that is more common in individuals with comorbid ID. Research into neurological and genetic causes of ASD is of strong clinical significance for understanding how and why neural circuitry differences manifest in these individuals and lead to neurodevelopmental disorders.

Neurological Correlates of ASD

Autism spectrum disorder has clear neurological correlates. Relative to typically-developing controls, children with ASD demonstrate abnormally rapid increases in overall brain size. Examination of the medical records of 99 infants aged 2-5 years (40 with ASD, 9 with PDD, 51 normally-developing controls) showed ASD diagnosis was associated with smaller-than-average head circumference at birth, that increased to significantly larger-than-average head circumference at 6-14 months (Courchesne, Carper & Akshoomoff, 2003). This appears to indicate an initial brain mass deficit that is followed by neural overgrowth in infancy (Courchesne et al., 2003). This finding appears to be robust and is supported by a magnetic resonance imaging (MRI) study, showing that ASD diagnosis in children aged 3-4 is associated with significant enlargements of the cerebrum, cerebellum, hippocampus, and amygdalae relative to controls (Sparks et al., 2002). Results of this study were consistent in children with both average and lower-than-average intellectual functioning, suggesting that increased neural mass is common neurological ASD symptom across diverse intellectual phenotypes (Sparks et al., 2002). Increases in white matter mass have also been inferred in 7 children with ASD aged 1.8-3.3 years following diffusion tensor imaging (DTI) (Bashat et al., 2007).

The literature I reviewed suggests that neurological differences common to ASD are present at birth (Courchesne et al., 2003), so they may begin embryonically. Whilst these studies appear to suggest ASD is associated with an increase in the number of individual neurons and glia in the brain, they could also suggest a potential role of neuronal hyper-connectivity and functional changes in synaptogenesis during ASD development.

Genetic Causes of ASD and the Role of Shank

Identifying genetic causes of ASD, and their impacts on neurodevelopment, is a priority in current ASD research. A study of monozygotic and dizygotic twins containing at least one autistic proband demonstrated that the likelihood of twins developing ASD or similar functional deficits increased with genetic similarity (Bailey et al., 1995).

Mutations of the Shank gene family have consistently been implicated in epidemiological studies of ASD. First identified by Naisbitt et al. (1999) as a scaffold protein in the post-synaptic density of excitatory neurons, the Shank family comprises Shank1, Shank2, and Shank3 protein isoforms. Structural features of Shank proteins include a PDZ domain, proline-rich region, ankyrin-repeating domain, SH3 domain, and sterile alpha motif (SAM) domain, each of which may bind to and regulate the function of other proteins (Hayashi et al., 2009; Naisbitt et al., 1999; Sheng & Kim, 2000). Shank gene mutations are associated with diverse neurological phenotypes, which appear to be mediated according to the site and type of disruption, and the protein binding sites effected (Durand et al., 2011; Hamdan et al., 2011; LeBlond et al., 2014; Marshall et al., 2008; Monteiro & Feng, 2017).

The functional impairments of Shank-mediated ASD diagnoses are particularly pronounced when the Shank3 gene is mutated or protein production is impaired (i.e., haploinsufficiency) (Durand et al., 2011; Hamdan et al., 2011; LeBlond et al., 2014; Marhsall et al., 2008; Monteiro & Feng, 2017). For instance, Shank3 truncating mutation has been identified in an individual with ID and delayed language acquisition in a gene sequencing study (Hamdan et al., 2011). Perhaps the most salient example of Shank3 mutation is Phelan-McDermid syndrome, (Phelan & McDermid, 2009) a neurodevelopmental disorder associated with deletion of gene

22q13 on chromosome 22. This results in deletion of the entire Shank3 gene and endogenous knockout of Shank3 protein (Phelan & McDermid, 2009). Phelan-McDermid syndrome diagnosis is often comorbid with and includes common symptoms to ASD, including language delay, abnormal social behaviour, and abnormalities in body development, as well as neurological symptoms such as seizures, headache, sleep disturbance, and changes in sensory perception (Phelan & McDermid, 2009).

Behavioural and Neurological Consequences of Shank Mutation in Animal Studies

Gene editing techniques allow the introduction of known mutations to animal genotypes, and examination of resulting behavioural and neurological phenotypes. For instance, transfection of silencing RNA (siRNA) inhibits protein translation from messenger RNA and leads to protein knockdown (Bargmann & Gilliam, 2013). Introduced Shank gene mutations are associated with autistic-like behavioural phenotypes in vivo, as well as abnormalities in neural transmission that appear to be specific to the isoform targeted.

Using immunocytochemistry, Wu et al. (2017) showed that Shank protein localises in the presynaptic neuromuscular junction of drosophila brains. Following various Shank mutations, synaptogenesis in the larval calyx was reduced, but subsequently rescued by transfection of an unmutated Shank gene sequence. Relative to controls, Shank-mutant drosophila displayed impaired performance on climbing assays, T-mazes, and motor and learning tasks, that was subsequently restored following transfection of unmutated Shank. As such, behavioural and neurological impairments in this study were shown to be specific to targeting of the Shank gene.

Shank1 Mutation

Shank1 KO mice show deficits in vocalisation when isolated from mothers, and abnormal scent marking behaviour in response to female urine, indicative of ASD-like abnormalities in social communication (Wöhr, Roullet, Hung, Sheng & Crawley, 2011).

Shank2 Mutation

Schmeisser et al. (2012) created homozygous and heterozygous Shank2 knockout (KO) mice. Homozygous mutants (lacking both copies of Shank2) were hyperactive, anxious, more likely to engage in repetitive behaviours (e.g., grooming), and showed social abnormality relative to controls. Golgi staining revealed reduced dendritic spine density in CA1 hippocampal cells of homozygous KO mice relative to controls. Homozygous KO was associated with upregulation of Shank3 protein throughout the striatum, hippocampus, and cortex, as well as significant upregulation of NMDAR subunit GluN1, and improved NMDA-mediated LTP in Shank2 KO mice. However, overall glutaminergic transmission was impaired, with reduced overall frequency of excitatory post-synaptic potentials (EPSPs). The increased abnormal behaviour and neuronal pathology in homozygous mutants indicates that haploinsufficiency of Shank2 protein is associated with greater functional deficits and neuronal pathology.

Zaslavsky et al. (2012) demonstrated that induced pluripotent stem cells containing various ASD-associated Shank2 mutations demonstrated increased axonal branching and synaptogenesis compared to unmutated controls, and greater frequency of excitatory post-synaptic currents. This research suggests a potential role of Shank2 as a branching antagonist and inhibitor of neural activity.

Shank3 Mutation

Zhou et al. (2019) used CRISP_R to introduce known ASD-associated Shank3 mutations in macaque embryos. Compared to age- and sex-matched controls, gene-edited macaques displayed ASD-like behaviours including increased sleep disturbance, reduced arm muscle strength, abnormal social behaviour, and engagement in repetitive behaviours such as excessive grooming. Neuroimaging methods including MRI showed reductions in grey matter in gene-edited macaques compared to controls, as well as reduced connectivity in the default mode network and thalamus, and greater connectivity in the somatosensory cortex. This indicates abnormalities in neural circuitry that may alter processing in the sensory system, which may be inferred to underlie ASD symptoms like auditory hypersensitivity (American Psychological Association, 2013). An effect of Shank mutation on abnormal sensory processing appears to be likely, as Shank 1, 2, and 3-deficient mice and rats demonstrate deficient nociception following sharp pain, heat pain, and chronic pain (Han et al., 2016; Miletic, Dumitrascu, Honstad, Micic & Miletic, 2010; Yoon et al., 2017). Following Shank3 KO in mice, deficits in pain-like behaviour have been associated with reduced activity in spinal cord neurons and deficient activation of heat-pain receptors (Han et al., 2016).

Durand et al. (2012) transfected cultures of human embryonic kidney (HEK) and COS-7 (monkey kidney) cells with various Shank3 mutations observed in specific ASD patients. With regards to the actin cytoskeleton, wild type Shank3 ($Shank3^{WT}$) localised in the actin filaments of HEK cells, but Shank3 mutated isoforms did not. In a co-immunoprecipitation assay, over-expressing $Shank3^{WT}$ increased F Actin production. This suggests that Shank3 colocalises with and acts on the actin cytoskeleton. With regards to cellular activity and morphology,

overexpressing Shank3^{WT} in hippocampal neurons increased dendritic spine formation and spine head size, whereas hippocampal cells transfected with GFP-tagged Shank3 mutations had reduced amplitude and frequency of excitatory post synaptic potentials compared to controls.

In a study of neural correlates of Shank3 haploinsufficiency, Bozdagi et al. (2010) created heterozygous mutant mice lacking the ankyrin-repeating domain of the Shank3 protein. Shank3 haploinsufficiency was associated with deficient GluR1 immunofluorescent puncta in immunohistochemical analysis of 3-4 month postnatal brain slices, indicating reduced number of synaptic AMPA receptors. In a patch-clamp recording procedure of basal cellular activity, weaker EPSP activity was recorded in hippocampal CA1 neurons from mutant animals. At 2 hours post induced tetanus, LTP maintenance was impaired, and mutant cells failed to grow dendritic spines that would be necessary for functional connectivity in vivo. This suggests that Shank3 haploinsufficiency reduces synaptic formation of AMPA receptors, which in turn reduces electrical signalling and aberrations in cellular morphology. Furthermore, male Shank3 mutant mice displayed abnormal social behaviour including reduced anogenital and nose-to-nose sniffing of a female mouse compared to controls, and reduced ultrasonic vocalisation.

Peça et al. (2011) created Shank3 mutant mice lacking PDZ domain binding sites. Shank3 mutant mice displayed abnormal social behaviour and increased anxiety in protocols like the open field test, as well as increased self-grooming, likelihood to experience seizures during routine handling, and self-injurious behaviour. Western Blot analysis showed reduced density of Homer1b/c and several glutaminergic proteins in striatal tissue of mutated mice compared to controls, indicating a potential role of full-length Shank3 in regulating protein formation.

Shank3 mutant mice also had increased caudate volume and reduced overall electrical activity in caudate-striatal tissue.

The current literature is consistent with a narrative of Shank3 protein inducing LTP-based cellular morphological changes. Roussignol et al. (2005) demonstrated that pan-Shank protein was expressed in the dendritic spines of cultured hippocampal cells, and that small interfering RNA (siRNA)-mediated Shank3 knockdown reduced overall Shank immunoreactivity and was associated with decreased spine density. Furthermore, transfection of Shank3 led to dendritic spine growth in aspiny cerebellar granular cells, and was associated with increased density of ionotropic NMDA and AMPA receptors, greater mGluR1 immunoreactivity, and greater NMDA- and AMPA-mediated basal electrical activity. It appears that Shank acts in tandem with Homer1 and metabotropic glutamate receptors to cause these changes, as transfection with Shank3 mutant plasmids lacking Homer1 and PSD-95 binding sites reduced localisation of pan-Shank protein in spines, and reduced the number of mGluR1-reactive puncta.

This literature indicates pan-Shank functions in the regulation of neural signalling, and supports the hypothesis that abnormalities in neural connection and synaptic transmission underlie autistic behaviour. In particular, Shank protein isoforms appear to work with Homer to regulate LTP, synaptogenesis, and glutaminergic signalling (Roussignol et al., 2005).

The Role of Shank Protein in Embryonic Development

The literature reviewed suggests a role of Shank gene in determining mature neuronal morphology and activity level, but there is currently a dearth of research into the potential role of Shank during synapse formation in embryo. This is surprising for several reasons. Firstly, ASD-associated Shank mutations are heritable

and well documented, and have robust neurological and behavioural consequences in the literature reviewed. Secondly, the seminal study that identified Shank in the post-synaptic density also found an unspecified Shank isoform in the growth cones of cultured hippocampal neurons (Naisbitt et al., 1999). Shank3 has since been identified in growth cones of cultured hippocampal neurons by Durand et al. (2012), within which neurons transfected with GFP-Shank3^{WT} displayed greater growth cone motility than cells transfected with mutated Shank3. Thirdly, Shank binds to Homer at the proline-rich domain of mature neurons (Tu et al., 1999), a protein that regulates intracellular responses to excitatory neurotransmitters and is necessary for ordinary BDNF and Netrin-mediated cellular activity (Gasperini, Choi-Lundberg, Thompson, Mitchell & Foa, 2009). I therefore asked whether Shank3 regulates the circuit formation of embryonic neurons in vitro via intracellular signalling processes.

Links to Homer

Homer1 proteins comprise Homer1a and Homer 1b/c isoforms, all of which are capable of binding to IP_3 and glutamate receptors (Tu et al., 1998). The crystal structure of Homer1a comprises an Ena/VASP homology 1 (EVH1) domain only (Hayashi et al., 2009), and is upregulated by neuronal excitation in the form of induced seizures (Brakeman et al., 1997). Homer1b/c isoforms contain an EVH1 and coiled-coil domain (Brakeman et al., 1997; Hayashi et al., 2009). Hayashi et al. (2009) demonstrated that Shank1 binds to Homer1b in the coiled-coil region, referred to this structure as a tetramer, and demonstrated that transfection of mutations to the Homer1b coiled-coil domain (to inhibit Shank1-Homer1b binding) was associated with reduced ability of CA1 hippocampal cells to form dendritic spines, and reduced NMDA- and AMPA-mediated excitatory post-synaptic current. This research showed that binding of Homer1b and Shank1 is necessary for ordinary

dendritic morphology and electrical activity in vitro. It is possible that a regulatory role of Shank-Homer tetramers extends to other cell types that co-express Shank and Homer isoforms in vivo.

The Growth Cone

The growth cone is a structure on the distal tip of developing axons comprised of a central zone (containing microtubules) and a peripheral zone (containing filopodia and lamellopodia) (Zheng & Poo, 2007). Filopodia use chemoattractants and contact cues to guide cell motility, which is ultimately made possible by structural reorganisation of the growth cone (Zheng & Poo, 2007). Lin and Forscher (1993) used sea slug bag cell neurons as a model organism to demonstrate growth cone motility by fixing and staining cells at varying stages after cell-cell contact. Following filopodial contact cues, the growth cone moved its actin and organelles to the contact site to initiate turning. This was followed by turning of the two central zones, and movement of the microtubules from a fan-like complex to a set of parallel tubules at the contact site.

Embryonic dorsal root ganglia (DRG) growth cones are excitatory pseudo-unipolar cells of the peripheral nervous system (PNS). Cell cultures of embryonic Sprague-Dawley DRG were selected as the model cell type for this study, for two reasons. Firstly, embryonic DRG growth cones have consistent and well-documented attractive responses to neurotrophic factors including nerve growth factor (NGF) (Gundersen & Barrett, 1980) and brain-derived neurotrophic factor (BDNF) (Gasperini et al., 2009), and repulsive responses to semaphorin-3a (Pavez et al., 2019; Gasperini et al., 2009; Mitchell, Gasperini, Small & Foa, 2012**)** and collapsin (Fan & Raper, 1995), and have been used within our laboratory to infer the effects of transfected gene knockdowns on calcium-mediated and calcium-independent cellular

signalling (e.g. Pavez et al., 2019; Gasperini et al., 2009; Mitchell et al., 2012). Cell cultures of embryonic DRGs prepared within our laboratory typically develop axons with large, fan-like growth cones within 4-6 hours post-plating, allowing for motility assay experimentation within 1 day of dissection (see Mitchell et al., 2012).

Secondly, Shank has previously been localised in mouse and rat DRGs in studies of protein haploinsufficiency and nociception. Miletic et al. (2010) describe upregulation of Shank1 protein in Sprague-Dawley rat DRGs following ligation of the sciatic nerve. Anisomycin injection (that inhibits translation of Shank1) was associated with decreased preferential weight-bearing in ligated animals, indicating decreased nociception. This means that Shank protein is present in the DRGs of mature rats, is necessary for sensory perception, and may therefore be present in embryonic DRG growth cones. Furthermore, extensive immunocytochemical analyses by Han et al. (2016) showed immunoreactive Shank3 protein in both pre- and post-synaptic areas of the spinal cord. The authors isolated Shank3 protein in the DRGs of mice, rats, and humans, and used patch-clamp recordings to identify deficient cellular responses to capsaicin (and associated reduced behavioural pain responses) in Shank3 knockout animals.

The Effects of Glutamate and BDNF-binding on Intracellular Signalling

Jessell and Sanes (2013) extensively reviewed the intracellular signalling pathways that occur following activation of metabotropic glutamate receptors (mGluRs) on the cell membrane. Following binding of glutamate to mGluR1, activated phospholipase C transforms phosphatidylinositol (4,5)-bisphosphate (PIP_2) to diacylglycerol (DAG) and Inositol 1, 4, 5 triphosphate (IP_3). Binding of IP_3 to IP_3 receptors on the endoplasmic reticulum (ER) stimulates calcium release. Calcium-mediated activation of calcium-calmodulin-dependent protein kinase II (CaMKII)

then occurs, which has been implicated in attractive growth cone turning (Wen, Guirland, Ming & Zheng, 2004). Reichdart (2006) describes similar activation of Phospholipase C and resulting calcium release following binding of nerve growth factor (NGF) and brain derived neurotrophic factor (BDNF) to the Trk-A and Trk-B receptors, respectively. As such, neurotrophic factors including both glutamate and BDNF are implicated in a complex network of intracellular signalling that underlies calcium release.

Mutated forms of Shank protein have the potential to disrupt BDNF-mediated calcium release within the IP_3 signalling pathway. Gasperini et al. (2009) demonstrated that Homer mediates ER-calcium release, and suggested that this occurs via Homer binding to TRPC channels on the ER membrane (demonstrated in Yuan et al., 2003). As such, Homer may potentially regulate both glutaminergic and BDNF-mediated calcium signalling through action on the IP_3 signalling pathway. As Shank-Homer tetramers have been shown to be necessary for mature neuronal function (Hayashi et al., 2009; Tu et al., 1999) there is potential that disrupting Shank-Homer binding may also disrupt the ability of Homer to regulate IP_3-mediated signalling.

Calcium Regulates Growth Cone Motility

Neuronal motility is calcium-dependent. Rises in intracellular calcium (whether via calcium influx through membrane receptors, or release from the endoplasmic reticulum (ER)) within a specific range encourage axonal extension, but fluctuations in calcium outside of this range inhibit outgrowth (Kater & Mills, 1991). Wen et al. (2004) state that this is because large intracellular calcium increases stimulate CaMK-II to facilitate attraction, whereas smaller increases activate calcineurin (CaN), a repulsive intracellular cue.

Attractive and repulsive growth cone turning are disrupted following transfected knockdown of proteins that regulate ER-mediated calcium release. Gasperini et al. (2009) used live cell imaging techniques to demonstrate the effects of morphelino-mediated Homer1b/c knockdown on growth cone motility in DRGs. In a turning assay, Homer1b/c knockdown reversed the response to BDNF and Netrin-1 from growth cone attraction to repulsion, indicating disruption to intracellular signalling pathways. Follow-up calcium imaging revealed that calcium spikes were reduced in oligo-treated growth cones, an aforementioned cause of cellular repulsion (Kater & Mills, 1991). Application of thapsigargin was associated with ER-emptying in oligo-treated but not control cells that had previously been exposed to BDNF. This suggests that Homer1b/c knockdown inhibited BDNF-induced ER-calcium release, and suggests that by regulating response to BDNF (and thus, calcium release), Homer1b/c regulates cell motility. Follow-up Western Blot and immunocytochemistry analysis showed that Homer1b/c colocalises with Stim1 and TRPC, proteins that further regulate calcium release.

Given that Shank has been localised in the growth cone (Naisbitt et al., 1999), mutation of Shank is associated with deficits in neurological signalling, and Shank binds with Homer at the proline-rich domain in mature neurons (Hayashi et al., 2009; Tu et al., 1999), I asked whether Shank protein was involved in guiding growth cone motility via Homer1b/c. In a continuation of the work by Gasperini et al. (2009), it was hypothesised that Shank knockdown would disrupt BDNF-mediated growth cone turning.

Aims and Hypotheses

Clarifying the neurodevelopmental role of Shank will shed light on whether disorders associated with Shank mutation may result from abnormal cell motility and

resulting abnormal neural circuit formation. The aim of this research is to determine whether Shank3 protein haploinsufficiency leads to aberrant growth cone turning in response to BDNF, and whether this may be due to functional binding with Homer1b/c in the growth cone. For this study, there were three hypotheses, each of which corresponds to a specific experiment.

Firstly, it was hypothesised that Shank and Homer 1b/c would colocalise within the growth cones of embryonic DRGs, as evidenced by overlaying immunoreactivity after immunostaining Shank and Homer with 594 and 647-tagged secondary antibodies, respectively. Given that Homer-Shank tetramers interact in vitro to regulate mature cell morphology and activity (Hayashi et al., 2009), colocalization in the growth cone may suggest protein-protein binding and interaction during neurodevelopment.

Secondly, following siRNA-mediated Shank3 knockdown, immunocytochemistry analyses would demonstrate a significant decrease in overall Shank immunoreactivity in cell somas and growth cones, as compared to wild type (WT) control cells untreated by siRNA. Significant differences in immunoreactivity would be consistent across a minimum of 3 repetitions of the same knockdown experiment.

Thirdly, growth cone turning response to BDNF would be significantly attenuated in growth cones derived from siRNA-treated cultures. It was hypothesised that during a 30-minute turning assay, WT control growth cones would grow towards a gradient of BDNF exuded from a micropipette placed 70 microns and 45 degrees from the growth cone. In contrast, cells triturated with Shank3 siRNA were expected to demonstrate either attenuated or abolished turning responses.

After testing these three hypotheses, it should be possible to infer whether Shank3 protein is involved in BDNF-dependent growth cone motility in vitro. The experiments conducted within this study also explore the possibility that Homer1b/c and Shank3 proteins work in tandem to regulate ER-mediated calcium release via the IP_3 pathway.

Materials and Methods

Animals

All procedures were carried out in accordance with National Health and Medical Research Council ethics guidelines following approval from the Tasmanian Animal Ethics Committee. At 18.5 days post-fertilisation (E18.5), pregnant Sprague-Dawley rats ($N = 25$) were euthanised via CO_2 inhalation by a competent laboratory staff member, and checked for reflexes to ensure animals were deceased. Embryos ($N = 58$) were then removed and decapitated in a petri dish using sterile forceps.

Cell Culture

Embryos were kept on ice prior to dissection. Skin and spinal cords were removed from embryos using sterile forceps to reveal DRGs. These were then dissected into Earle's Balanced Salt Solution (EBSS; Gibco) and placed in 200ul aliquots of Sensory Neuron Media (SNM). Cells were then triturated and plated directly onto coverslips, or left in 1ml SNM overnight at 5ºC.

Transfection

Shank3 knockdown was achieved by triturating cells 10-20 times in 200ul SNM with 2ul Shank3 siRNA (Thermo Fisher Scientific, Cat# s133190). Wild type (WT) cells were triturated without siRNA. Cells were then plated onto coverslips that had been nitric acid washed, pre-treated with polyornithine (PORN) (250ul 10mg/ml PORN stock in 2250ul pure MilliQ water), UV cycled for 20 minutes, and coated with 50-100ul of 1mg/ml laminin solution (50ul laminin stock in 950ul Tris/NaCl). Cells were grown at 37ºC in a 95% air/5% CO_2 humidified incubator for >12 hours, and fed with 1ml of SNM 1 hour after plating.

Immunocytochemistry

After >12 hours incubation, cells were fixed for a minimum of 10 minutes in 4% paraformaldehyde solution (PFA) and then rinsed three times for 10 minutes using phosphate buffered solution (PBS; pH 7.5). Cells were blocked and permeabilised in a solution comprising 0.4% Triton-X-100 (Sigma-Aldritch) with 5% Normal Goat Serum (NGS) or Sheep Serum (SS) in PBS. Primary antibodies for immunocytochemistry were anti-Homer 1b/c (rabbit, 1:200; Cat#160023, Synaptic Systems) and anti-PAN-Shank (mouse, 1:200; Cat#S23b-49, Gene Tex) diluted in PBS with 5% NGS or Sheep Serum. Coverslips were incubated in primary antibody solution at 5ºC overnight then rinsed with three PBS rinses. Secondary antibodies were Alexa fluor 647 anti-Rabbit (1:1000), Alexa fluor anti-mouse 568 (1:1000), Alexa Fluor anti-mouse 594 (1:1000), Alexa Fluor Phalloidin 488 (1:200), and Hoescht Staining Dye Solution (1:10000, Cat#33342), which were bath-applied to cells in a darkened box for two hours and diluted in a PBS solution with 5% NGS or SS. Secondary antibodies were then removed from coverslips, which were rinsed three times in PBS, air dried, and mounted in DPX (Sigma-Aldrich) on glass microscope slides.

Live Cell Imaging

Procedures for coverslip preparation and knockdown are as described above. Coverslips for growth cone turning were glued to plastic turning dishes and cells were plated in 200ul SNM, left to grow for 12 hours, then fed with 2ml SNM directly prior to turning.

Chemoattractants used for turning were brain derived neurotrophic factor (BDNF) or control fluid (SNM). Live cell imaging was performed at 40x magnification on a turning rig. Chemoattractant-filled glass pipettes were placed at a 45º angle to

growth cones, at a distance of 70nm. Turning videos were comprised of 260 frames, taken once every 7 seconds for 30 minutes. Videos were retained for image analysis if cells extended a minimum of 10 microns over 30 minutes and had uncollapsed growth cones with visible filopodia and lamellipodia.

Microscopy

Immunofluorescent images for Shank3 knockdown experiments were acquired on an Olympus BX50 microscope using a 60x water immersion lens. Coverslips were searched systematically (left to right, top to bottom) for DRGs with axons and growth cones. Immunofluorescence for green (F actin, 500ms light exposure), red (Shank, 500ms light exposure) and blue (nuclei, 10ms light exposure) channels was captured using NIS elements software and a CCD camera (Photometrics, USA). Individual cells were selected for analysis by identifying DRG nuclei by Dapi immunoreactivity, and then confirming pseudo-unipolar morphology with an F-actin stain. Images of cells with axons and growth cones were taken preferentially due to the focus of this project on the neuronal growth cone. In situations where coverslips did not contain cells with axons and growth cones, cells with a visible F-actin cytoskeleton and nucleus were captured for somatic Shank analysis. Images were saved as stack ND2 files on a server accessible to researchers within the molecular neurobiology laboratory.

Immunofluorescent images for Shank and Homer immunocytochemistry were captured on a PE Spinning Disk microscope using channels FITC to identify F Actin fluorescence, TRITC to identify Homer1b/c, and CY5 to identify pan-Shank. Dorsal root ganglia soma and growth cones were identified as described above. Raw data were saved as stack TIF files on the laboratory server.

Image Analysis for Immunocytochemistry Experiments

The image analysis program Fiji (NIH) was used to quantify colocalization of Homer1b/c and pan-Shank protein in the growth cone. Stack images were split according to colour channel, and stack images were flattened. Homer1b/c was labelled in red and pan-Shank and F Actin were relabelled in green and cyan, respectively. Merged red and green (with resultant yellow coloration) were interpreted as evidence of Homer1b/c and pan-Shank colocalization.

Shank knockdown was quantified in the soma and growth cones of DRGs using Fiji. For knockdown analyses, stack images (16-bit) were split by colour channel and the red channel (Shank) was selected. Pixel intensity in the soma and growth cone was calculated by drawing around areas of interest, and measuring the integrated density of red immunoreactive pixels. In order to calculate differences in immunofluorescence between areas of protein fluorescence and areas of background, I analysed pixel density in cell soma (N = 30) and equivalent-sized sections of black background (N = 30) from WT (N = 30) cell images. This revealed that protein fluorescence was greater in soma (M = 7.53e+7, SD = 4.52e+7) than in background (M = 2.67e+7, SD = 1.97e+7). As such, reductions in Shank3 expression in the soma should be indicated by reduced integrated density measurements (i.e., more black background).

Design and Statistical Analysis for Knockdown Experiments

Shank3 knockdown experiments were comprised of two independent variables (IVs). The first IV, treatment group, had two levels: siRNA-mediated knockdown cells (KD) and wild-type cells (WT). Knockdown experiments were performed at three different time points, using embryonic DRGs from three different

pregnant animals. As such, experiment number was included as a second IV with three levels: Experiment 1, Experiment 2, and Experiment 3.

A 2 x 3 between subjects ANOVA was performed in Jamovi to analyse differences in somatic Shank immunoreactivity between KD and WT cells. A priori power analysis for 2 x 3 ANOVA was computed in G power, and indicated that a sample size of 27 items per condition (N=162) was required to find a moderate effect size at 80% power with alpha values set at .05. Although I originally planned to analyse growth cones with this method, soma were analysed because as cultures did not grow sufficient growth cones to power a 2 x 3 ANOVA.

Design and Statistical Analysis for Turning Experiments

All turning data calculations were performed in the image analysis program, Fiji (NIH). Turning angle (calculated with the angle tool) and extension (calculated with the line tool) were calculated in microns at two time points – in frame 1 (prior to chemoattractant exposure), and frame 260 (after 30 minutes of chemoattractant exposure). As such, independent variables were time (Frame 1, Frame 260), chemoattractant (BDNF, SNM control) and cell treatment group (KD, WT). Dependent variables were growth cone extension (microns) and turning angle (degrees). I therefore planned to analyse turning data in SPSS using MANOVA. A priori power calculation in G Power indicated that to achieve 80% power for a 2x2x2 MANOVA, with p<.05, a minimum sample size of 120 growth cones was required.

Results

Shank and Homer 1b/c Colocalize in Dorsal Root Ganglia Growth Cones

As Shank and Homer colocalize in mature neurons (Tu et al., 1999), and Homer1b/c has been identified as a regulator of ER-calcium release and growth cone motility (Gasperini et al., 2009), I hypothesised that Shank and Homer1b/c proteins would colocalise in DRG growth cones. Consistent with this hypothesis, merging green (Shank) and red (Homer1b/c) channels during image analysis was associated with a pattern of yellow coloration in merged images of the growth cone, indicating colocalization (see Figure 1E). Shank and Homer1b/c protein expression appears to be strongest in the axon and central region of the growth cone, with weaker immunoreactivity in filopodia and lamellopodia (See Figure 1A-D). However, this result should be interpreted with caution due to large amounts of red background in Homer1b/c staining.

Interestingly, merging green (Shank) and cyan (F Actin) colour channels was associated with an aquamarine coloration pattern in merged images of the growth cone. This suggests that Shank colocalizes with F Actin in the central region of the growth cone, and in the distal tips of filopodia (see Figure 1E).

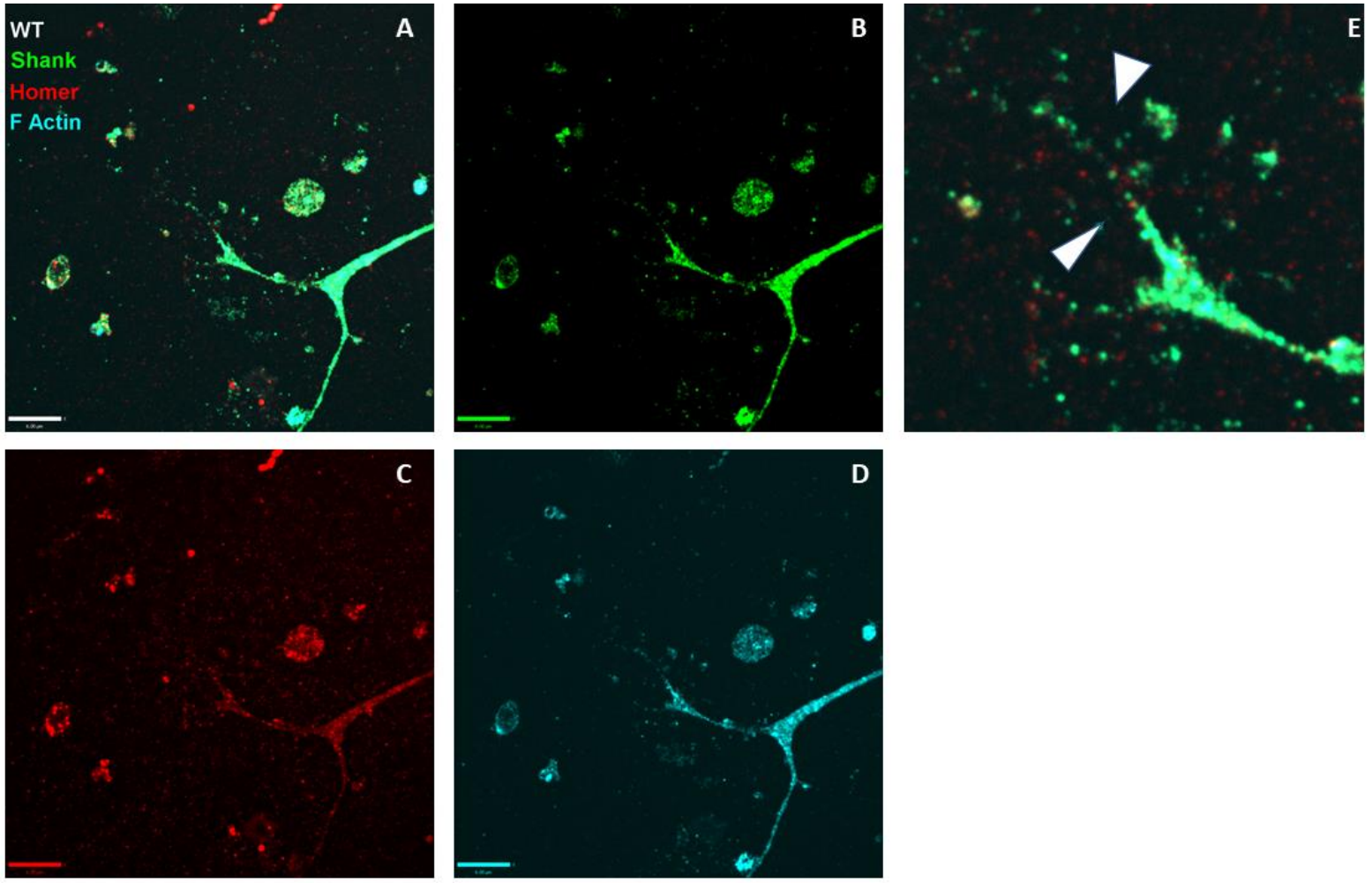
WT
Shank
Homer
F Actin
A
B
E
C
D

Figure 1.(A) Colocalisation (yellow) of Shank (Green) and Homer1b/c (Red) protein in the dorsal root ganglia axon and growth cone (B-D) Dorsal root ganglia axon and growth cone expressing Homer 1b/c (Red), F Actin (Cyan), and pan-Shank (Green) protein. (E) Close up image of F Actin, Homer1b/c and pan-Shank expression in the growth cone, showing colocalization (yellow) of Shank and Homer1b/c. Filopodia indicated by arrows.

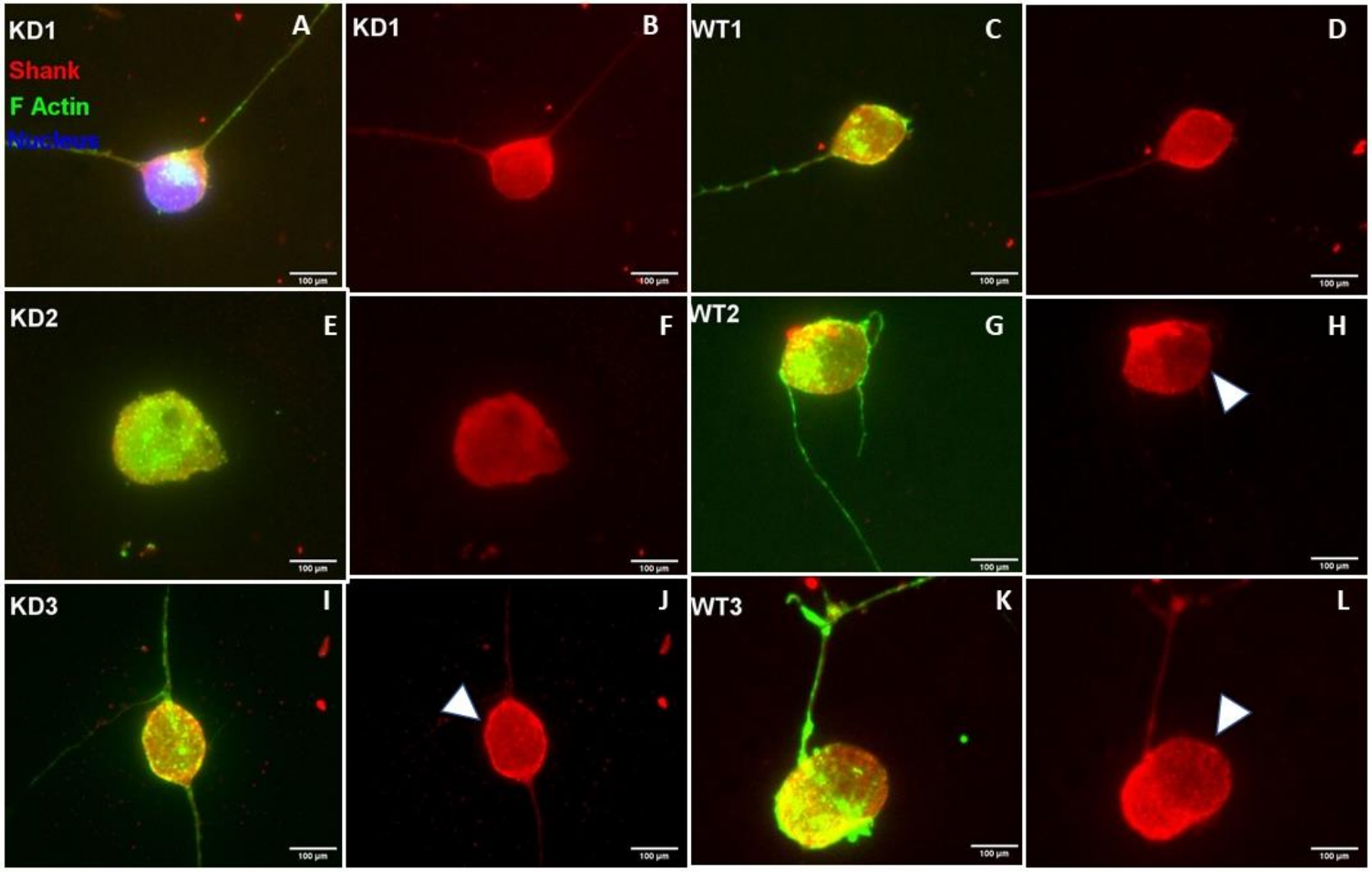
KD1
A
Shank
F Actin
Nucleus
KD1
B
WT1
C
D
KD2
E
F
WT2
G
H
KD3
I
J
WT3
K
L
100 µm

Figure 2. (A) Image of DRG soma showing nucleus (blue), Shank protein (red), and F-Actin cytoskeleton (green).(C, E, G, I, K) Colocalization (yellow) of somatic pan-Shank protein and F Actin. (B, D, F, H, J, L) Somatic Pan-Shank protein in wild type and siRNA-treated dorsal root ganglia. Arrows indicate reduced pan-Shank expression in the nucleus.

There was no Significant Effect of siRNA-mediated Shank3 Knockdown on Somatic pan-Shank Immunoreactivity

In order to test the second hypothesis, Shank3 knockdown was quantified in DRG somas. Immunocytochemical stains revealed that pan-Shank protein was enriched in the soma of both siRNA-treated and control DRGs and appeared to colocalize with F Actin (see Figures 2C, 2E, 2G, 2I & 2K). Pan-Shank immunoreactivity appeared to be weaker in the nucleus (see Figure 2H, 2J, and 2L).

Somatic knockdown of Shank3 protein was quantified using a 2 x 3 ANOVA. Data screening was performed to verify that assumptions of ANOVA were met, including normality, independence of observations, and homogeneity of variance. Cells were nested in coverslips, which may have undermined independence. Levene's test was non-significant, F (5, 156) = 2.15, p = .062, indicating the assumption of homogeneity of variance was not violated. The assumption of normality appeared to have been violated in raw data histograms (See Appendix 1). Therefore, raw integrated density scores were transformed using the natural logarithm function, and the ANOVA was performed on log scores. Following transformation, histograms revealed reductions in data skew and outliers indicating improved normality, and residuals approached normal distribution in a Q-Q plot. However, Levene's test was significant, F (5, 156) = 4.43, p < .001, indicating heterogeneity of variance. As such, results should be interpreted with caution.

Table 1

Descriptive Statistics for Somatic Pan-Shank Immunoreactivity in Knockdown and Wild Type Cells, prior to Log Transformation

Treatment Group	Experiment Number	Sample Size	Mean Integrated Density	Median Integrated Density	Standard Deviation	95% Confidence Interval
Knockdown (KD)	1	27	8.04e+7	8.12e+7	2.97e+7	6.31e+7, 9.77e+7
	2	27	6.54e+7	5.40e+7	5.15e+7	4.81e+7, 8.28e+7
	3	27	7.96e+7	8.63e+7	3.55e+7	6.23e+7, 9.70e+7
	Overall	81	7.52e+7	7.34e+7	4.01e+7	6.51e+7, 8.52e+7
Wild Type (WT)	1	27	6.90e+7	8.45e+7	3.76e+7	5.17e+7, 8.64e+7
	2	27	7.02e+7	5.74e+7	5.78e+7	5.29e+7, 8.76e+7
	3	27	6.87e+7	5.79e+7	5.41e+7	5.14e+7, 8.61e+7
	Overall	81	6.93e+7	6.16e+7	5.00e+7	5.93e+7, 7.93e+7
			Marginal Mean			
	1	54	7.47e+7	8.15e+7	3.40e+7	6.24e+7, 8.70e+7
	2	54	6.78e+7	5.52e+7	5.43e+7	5.56e+7, 8.01e+7
	3	54	7.42e+7	6.48e+7	4.57e+7	6.19e+7, 8.64e+7

Log-transformed scores were analysed with a 2 x 3 ANOVA. Analysis of the main effect of treatment group revealed a small but nonsignificant increase in integrated pan-Shank pixel density in KD compared to WT cell somas, F (1, 156) = 1.67, p = .080, η^2_p = .02. (See Table 1). The nonsignificant result means that pan-Shank immunoreactivity in the cell soma was consistent across KD and WT treatment groups.

There was a small but non-significant main effect of experiment number on pixel density, F (2, 156) = 2.48, p = .087, η^2_p = .03. (See Table 1). This means there were no significant differences in Shank immunoreactivity across the three repetitions of the experiment, meaning results were consistent. Due to the lack of significance, post-hoc tests were not performed.

There was no significant interaction between experiment number and treatment group, F (2, 156) = 0.38, p =.337, η^2_p = <.01. This means that the non-significant effect of siRNA treatment was consistent across all three experiments.

There was no Significant Effect of Shank3 Knockdown on pan-Shank Expression in the Growth Gone

In order to verify that non-significant knockdown effects were not soma-specific, I performed follow-up analyses quantifying the effect of Shank3 knockdown on pan-Shank immunoreactivity the growth cone. Of the 162 cells tested originally, 52 grew growth cones. Pan-Shank immunoreactivity was evident in both collapsed and uncollapsed growth cones across all three experiments and treatment groups (see Figure 3).

I quantified the effects of Shank3 knockdown in KD and WT growth cones by calculating the integrated density of red immunoreactive pixels indicating filopodia and lamellopodia (see Figure 3). As the previous analysis demonstrated

that pan-Shank protein expression was consistent across the three experiments, treatment group (KD, WT) was included as the sole independent variable in this analysis.

I planned to compare pan-Shank immunoreactivity in KD and WT control growth cones using an independent samples *t* test. However, assumption checks revealed data were not normally distributed, and this was not rectified using log transformations. Untransformed scores were therefore analysed using a non-parametric Mann-Whitney U test with the hypothesis that integrated density of immunoreactive pixels would be unequal between WT and KD growth cones.

A Mann-Whitney U test revealed that pan-Shank immunoreactivity was slightly increased in WT growth cones (N = 29, M = 7.43e + 6, SD = 6.75e + 6), as compared to KD growth cones (N = 25, M = 5.96e + 6, SD = 2.79e + 6), U (52) = 357, p = .931, 95% CI [-2.83e - 6, 2.05e + 6], d = -.28. This represents a small-to-medium effect that was not statistically significant. However, results may be underpowered and should be interpreted with caution. A priori power analysis was not possible due to the reliance of this analysis on previously collected data.

The Effects of Shank3 Knockdown on Turning were not Quantifiable

In order to test the effects of Shank3 knockdown on growth cone motility and extension, I planned to capture 120 live cell turning videos, and analyse these with a 2 x 2 x 2 MANOVA. However, cell culture growth was insufficient to adequately power this analysis. Turning assays were attempted with KD and WT cell cultures on five separate sessions. Across all sessions, only 10 live cell videos (7 WT control) were captured. Of these, 4 were unsuitable for analysis due to collapsed growth cone morphology, failure of the growth cone to extend a minimum of 10 microns in 30 minutes, or incorrect angle of the growth cone to the pipette. As each testing session

required 3-6 hours, it was decided that the time commitment required for turning data collection was beyond the scope of this project.

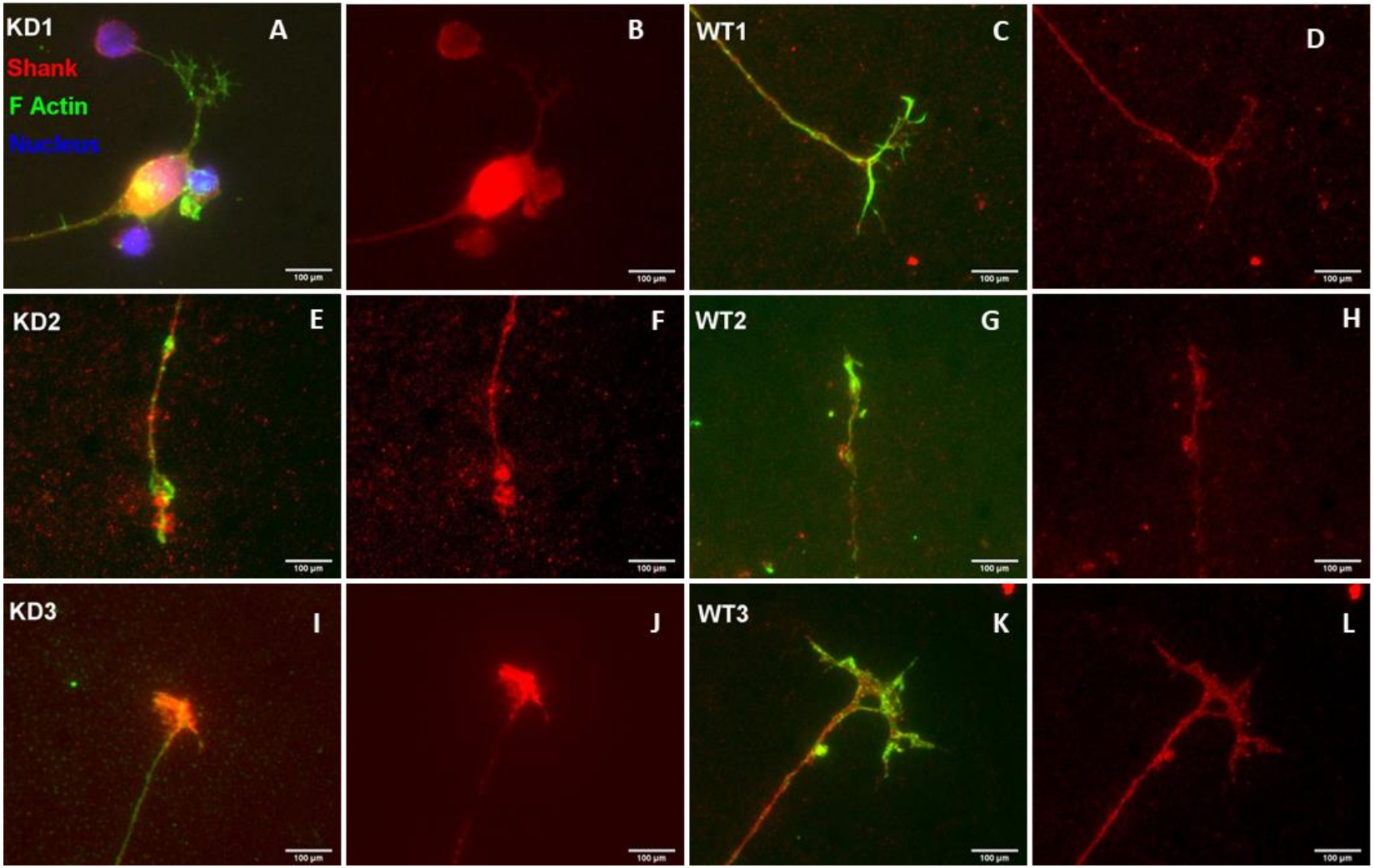
KD1
A
Shank
F Actin
Nucleus
B
WT1
C
D
KD2
E
F
WT2
G
H
KD3
I
J
WT3
K
L
100 µm

Figure 3.(A) Dorsal root ganglia with soma, nucleus (blue), axons, and growth cone expressing pan-Shank (red) protein and F actin (green). Pan-Shank immunoreactivity in the growth cones of siRNA-treated and wild type dorsal root ganglia. (C, K) Uncollapsed growth cones showing colocalization (yellow) of Shank protein with F Actin. (E, G, I) Collapsed WT and siRNA-treated growth cones. (B, D, F, H, J, L) Expression of pan-Shank protein in collapsed and uncollapsed siRNA-treated and WT growth cones.

There was no Significant Difference between Knockdown and Wild Type Cell Culture Growth

Failure to complete turning experiments was unexpected and necessitated re-evaluation of cell culture methodology and identification of potential confounds. During live cell imaging and immunocytochemistry experiments, naïve observation suggested that siRNA-treated DRGs appeared to grow fewer axons, and were more prone to collapse compared to wild type controls. I therefore asked whether Shank3 siRNA treatment reduced axonal growth. To test this hypothesis, and eliminate potential effects of my own inexperience on cell culture failure, a competent member of the laboratory group pre-prepared coverslips with WT DRG cell cultures (*N*=2), and cultures containing siRNA (*N = 2*). Using protocols described previously, I stained cultures for expression of F actin and nuclei. Microscopic analysis of growth cones was completed using a BX50 60x water lens. Due to the focus of this hypothesis on neural growth, only DRGs with a minimum of one axon were included for analysis (*N*=19).

For this experiment, there was a single IV (cell treatment group) with two levels (KD, WT control), and a single DV (number of growth cones). Data were analysed in Jamovi with an independent sample *t* test, revealing that there was no significant effect of siRNA treatment on the number of growth cones displayed by a cell, t (17) = .16, p = .879, d = .07, 95% CI [-.56, .65]. Wild type DRGs with growth cones (N = 10) grew a mean of 1.40 growth cones per cell (SD = .52), whereas KD DRGs with growth cones (N = 9) grew a mean of 1.44 growth cones per cell (SD = .73).

During turning assays, I also observed that the majority of growth cones in all cell cultures were collapsed (see Figure 3E & 3G). This was problematic, as

motile growth cones should display a fan-like, spreading morphology for turning assays to be viable (see Figure 3 images KD1, WT1, and WT3). I therefore asked whether growth cone morphology (collapsed, uncollapsed, or contacting another cell) differed from a random distribution within the sample of 19 DRGs analysed above.

A chi square goodness of fit test was used to examine the morphology of the first growth cone of every DRG (N = 19). Data were categorical and expected counts per cell were >5, meaning assumptions were met. Growth cone morphology types differed significantly from a random distribution, χ^2 (2) = 17.8, p <.001. Of the growth cones analysed, 15 were collapsed, two had made contact cues with other cells, and only two were uncollapsed and suitable for turning analysis.

In order to determine whether growth cone viability for turning assays was compromised by siRNA-treatment, I asked whether growth cones derived from KD cultures were more prone to collapse than WT growth cones. However, a chi square test of independence revealed that morphology of the first growth cone was not dependent on treatment group, χ^2 (2) =.01, p =.993, Kramer's V = .03. This means that the majority of growth cones were collapsed across both experimental and control groups.

Discussion

The aim of this study was to elucidate the function of Shank3 protein in the growth cone of developing DRG growth cones. It was hypothesised that knockdown of Shank3 would abolish turning in response to BDNF, a typically attractive neurotrophic factor. However, the current project was subject to ongoing cell culture issues that decreased the ability to elucidate functions of the Shank protein in vitro. As such, we did not find support for the alternative hypothesis that Shank3 knockdown would disrupt BDNF-induced turning, but equally cannot reject the null.

Pan Shank Protein is Present in the Growth Cones of Dorsal Root Ganglia and Colocalizes with Homer1b/c

Consistent with the first hypothesis, Shank protein was localised in the growth cones of DRGs and colocalised with Homer1b/c. This finding is clinically significant for several reasons.

Firstly, to my knowledge, the discovery of pan-Shank protein in the growth cones of DRGs is novel. Han et al. (2016) previously localised Shank3 protein in the DRG of rats, mice, and humans, and identified both pre- and post-synaptic functions of Shank3 in the spinal cord. Similarly, Miletic et al. (2010) implicated Shank1 in the regulation of pain signalling in mature DRGs. The current study suggests another role of Shank protein in the DRG, in embryonic axonal development. An unspecified Shank protein isoform (Naisbitt et al., 1999) and Shank3 protein (Durand et al., 2011) have both previously been localised in the growth cones of cultured hippocampal neurons, indicating a role of this protein in central nervous development. However, to my knowledge, this is also the first study to localise Shank protein in growth cones of the peripheral nervous system.

What does this mean for our understanding of Shank protein function in ASD? Firstly, this suggests a role of Shank protein in peripheral axonal projection. Interestingly, haploinsufficiency of all three Shank isoforms has been implicated in ASD-like phenotypes and deficient nociception in rodents (Han et al., 2016; Miletic et al., 2010; Yoon et al., 2017). A common symptom of ASD is abnormal sensory perception (American Psychological Association, 2013). If future research shows Shank haploinsufficiency reduces growth cone responsiveness to attractive neurotrophic signals in peripheral neurons, this may indicate that abnormal perceptive features of ASD are due to inability of peripheral sensory neurons to find CNS targets.

There is another potential implication of the current finding. I stained DRGs for pan-Shank immunoreactivity, and failed to confirm knockdown following treatment with Shank3 siRNA. As such, it is entirely possible that stains were reactive to Shank1 or Shank2 isoforms. The lack of Shank3 knockdown suggests that embryonic DRG development may involve Shank1 or Shank2 isoforms, whereas cellular signalling in mature DRGs appears to be regulated by Shank1 and Shank3 (as shown in Han et al., 2016 & Miletic et al. 2010). As specific isoform staining would be required to validate this hypothesis, a clearly defined question suitable for a future thesis project would be: does Shank isoform expression differ between DRG cultures derived from embryonic (i.e., E 18.5) and postnatal rats?

Consistent with the hypotheses, Shank colocalised with Homer1b/c in DRG growth cones. This finding aligns with research by Tu et al. (1999) showing colocalization of Shank and Homer proteins in developed neurons, but is novel in identifying colocalization in growth cones. Given that Homer1b/c has been shown to regulate axon pathfinding in vitro turning assays (Gasperini et al., 2009), and

functional binding of Shank and Homer1b/c is necessary for ordinary cellular activity (Hayashi et al., 2009), the presence of colocalization indicates a potential role of Homer-Shank tetramers in embryonic axon pathfinding. For instance, Homer1b/c mediated signalling may involve functional binding with Shank. However, follow up testing (e.g., completion of growth cone turning assays with Shank3 knockdown) would be necessary to explore this possibility.

Visual assessment methods of colocalization analysis have previously been criticised for observer bias (Costes et al., 2004). This is problematic, as I expected to find Homer1b/c and Shank colocalization prior to immunocytochemistry experiments, and likely interpreted results with confirmation bias. I recommend an unbiased correlational analysis of protein colocalization (as in Costes et al., 2004) to objectively measure the degree of association between Homer and Shank proteins and validate results. Alternatively, visual assessment of protein colocalization by multiple researchers ignorant to the hypotheses would reduce measurement bias and increase the internal validity of this experiment.

There was No Significant Difference in pan-Shank immunoreactivity between Shank3 siRNA-treated and Wild Type Cell Cultures

The current study failed to demonstrate knockdown of Shank3 protein in both the soma of DRG, and the growth cones. There are two reasons why knockdown may have been unsuccessful in these experiments.

Firstly, cells were transfected with Shank3-specific siRNA, but incubated in pan-Shank antibody. This method has previously been used to infer Shank3 knockdown as a decrease in overall Shank protein expression in cultures of aspiny cerebellar granular cells (Roussignol et al., 2005). As such, the lack of significant results in our study may reflect a difference in protein expression between cell types,

rather than an issue with the methodology. It is possible that embryonic DRGs express Shank1 or Shank2 isoforms, but not Shank3. This would have led to no difference in immunoreactivity between WT and KD cultures following Shank3 siRNA transfection. However, this would be unexpected, given that Shank3 protein has previously been isolated in mature DRGs by Han et al. (2016).

An alternative explanation is that downregulating production of the Shank3 protein isoform led to compensatory upregulation of Shank1 or Shank2, which could have led to no difference in overall Shank protein expression between KD and WT cells stained with pan-Shank antibodies. This is feasible, as Shank2 knockout in mice has previously been associated with increase in synaptic Shank3 protein (Schmeisser et al., 2012). If Shank3 haploinsufficiency leads to compensatory upregulation of other Shank isoforms, this would have reduced the interpretability of immunocytochemistry analyses that quantified Shank3 expression with pan-Shank primary antibody.

A third possible explanation is that an issue with the siRNA inhibited Shank3 knockdown. Consistent with manufacturer instructions, Shank3 siRNA was stored at - 20°C, and aliquots were refrigerated for a maximum of 2 weeks once thawed (Thermo Fisher Scientific, 2019). If siRNA knockdown ability decreased with time spent in a thawed state, this would have therefore been clearly demonstrated in the results as a gradual, systematic increase in pan-Shank immunoreactivity across both treatment groups from experiment 1 to experiment 3. However, there was no significant main effect of time in a 2x3 ANOVA, indicating that Shank expression was consistent across all three experiments.

Contrary to manufacturer guidelines (Thermo Fisher Scientific, 2019), cell cultures were incubated with siRNA for >12 hours post-transfection, instead of the

>24 hours recommended. This procedure was necessitated as growth cones were prone to collapse, but this procedure likely compromised internal validity by reducing the extent of Shank3 knockdown. A transfection period of 24-48 hours may therefore be more likely to yield significant knockdown results. However, based on the current dataset, it is unlikely that any growth cones would be uncollapsed after an incubation period of this length.

The use of a pan-Shank primary antibody made it impossible to determine which Shank isoforms were expressed in the growth cone. This represents a serious limitation. I therefore recommend repeating Shank3 knockdown in DRGs, but incubating WT and Shank3 siRNA-treated cells in Shank3-specific primary antibody to increase result specificity. As there was no significant effect of siRNA treatment on protein expression in the current study, I expect that DRG growth cones do not express Shank3 protein. This would explain the lack of significant results in knockdown experiments, and allow researchers to rule out alternative explanations like compensatory upregulation of other Shank isoforms, or lack of knockdown due to insufficient transfection time.

Limitations

Poor cell culture growth undermined live cell imaging procedures

It was impossible to quantify the effects of Shank3 knockdown on growth cone turning and extension. Both KD and WT cell cultures failed to grow sufficient growth cones to complete adequately-powered turning experiments, and the majority of growth cones observed in a follow-up immunocytochemistry protocol were collapsed. This result was consistent across both siRNA-treated and WT cells, meaning that Shank3 siRNA treatment did not differentially effect cell culture growth.

Growth cones collapsed during the >12 hour incubation period employed prior to live cell imaging. In the molecular neuroscience laboratory, immunocytochemical and live cell imaging data has previously been obtained from uncollapsed DRG growth cones within 4-6 hours post-plating (see Mitchell et al., 2012). An incubation period of this brevity was not feasible in the current experiment due to the transfection time required for siRNA knockdown (Thermo Fisher Scientific, 2019). However, examination of cell cultures during the incubation period revealed both siRNA-treated and WT cell cultures consistently failed to project axons even within 4-6 hours (data not shown). Other members of the laboratory did not experience similar issues with DRGs derived from the same animals, indicating that this issue was unique to my cultures. This indicates that I committed systematic errors throughout the experimental process that undermined the growth of both KD and WT DRGs.

Attempts to Improve Cell Culture Growth were Unsuccessful

When first alerted to issues with culture growth, I underwent complete retraining in coverslip preparation, dissection, and cell culture procedures. As many cultures contained bacteria, I ensured sterility by thoroughly spraying all dissection equipment and embryos with 70% ethanol solution prior to removing skin and spinal cords. This procedure successfully reduced bacterial growth, however, increases in DRG axonal projection were not observed.

Systematic errors in coverslip preparation may have reduced cell growth. Initially, I soaked coverslips in nitric acid for a minimum of one hour, then rinsed coverslips five times for 25 minutes with MilliQ H_2O. If rinses were insufficient to remove acid from coverslip glass, residual acid may have corroded cell cultures. To address this potential issue, I submerged coverslips in successive baths of nitric acid,

ethanol, and water to remove all acid and ensure glass sterility. This procedure increased the ability of SNM to form an airtight bubble over the coverslip (and thus, reduce exposure of plated cells to air). However, cell cultures still failed to grow axons and growth cones within the typical four hour period observed by other members of the laboratory.

This indicates that I committed errors, likely a result of inexperience, that led to cell death. To address this issue, a competent member of the laboratory group completed the coverslip preparation, dissection, and cell culture procedures for F-Actin-only analysis of DRGs. This allowed me to rule out inexperience at cell culture techniques as a factor effecting cell growth.

However, the growth of these cultures remained minimal, as four coverslips yielded only 19 DRGs with axonal growth – and of these, the majority of growth cones were collapsed. As axonal growth and growth cone collapse were not dependent on treatment condition, this indicates that errors in cell culture within the laboratory are systematic and are likely ingrained in the procedures used. Before continuing knockdown experiments, it is a priority to identify and rectify reasons for cell culture failure.

F-Actin immunostaining revealed that DRGs with axons were predominately multipolar. Clark, Britland, and Connolly (1993) demonstrated that DRGs grown without laminin are more likely to be multipolar, and increases in laminin concentration were associated with greater likelihood of bipolar cell morphology. As such, I propose that the lack of cell culture growth may have been caused by deficient laminin coating of coverslips. Increasing the amount of laminin stock in solution (i.e. from 1:20 parts to 1:10) may encourage axonal projection in future experiments.

Strengths of the Study

Shank3 knockdown quantification was region-specific

Shank3 knockdown was quantified in specific areas of interest (the soma and growth cone) using integrated pixel density analysis. This represents an improvement of traditional methods for quantifying knockdown, such as Western Blot, that quantify protein expression in an entire tissue sample (Alberts et al., 2015). Cell cultures in this study contained heterogenous neuronal, glial, and blood cells, of which pseudo-unipolar DRGs constituted only a small fraction, and DRGs with uncollapsed growth cones a smaller fraction still. Western Blot would have lacked the specificity necessary to quantify cell-specific (and indeed, growth-cone specific) knockdown in these cultures. Using region-specific analysis, I demonstrated that there was no significant difference due to siRNA treatment on Shank protein expression in the soma and growth cone of DRGs, a conclusion that could not have been made using Western Blot.

Knockdown results were consistent across three experiments

In order to increase internal validity, each knockdown experiment was repeated a minimum of three times, using embryonic DRG cell cultures derived from three different animals. In a 2 x 3 ANOVA, there was no significant main effect of experiment number on Shank protein expression, indicating results were consistent across all three testing sessions. This is a positive finding, as it means findings are likely to be robust, and experimental error was consistent across experiments. For instance, prolonged exposure to light during microscopy led to photobleaching of secondary antibodies. As such, a potential confound could have been that Experiment 1 microscopy (undertaken during the learning stage, when time required to take images was longer) was at increased risk of photobleaching. This could be

misinterpreted as decreased protein expression indicating knockdown success. However, as protein expression was consistent across all experiments, this eliminates photobleaching as a potential confound.

Rationalising the Choice of Statistical Analysis

The effects of Shank3 knockdown on protein expression should have been analysed with mixed linear modelling (MLM), as the ANOVA assumption of independence was violated. Data structure was hierarchical, with cells nested according to coverslip (Level 1 hierarchy), embryo (Level 2 hierarchy), and experiment number (Level 3 hierarchy). Whilst a 2 x 3 ANOVA indicated experimental consistency, it is possible that lower levels of the data hierarchy (i.e., coverslip conditions) influenced culture growth, as the rate of axonal projection was highly varied across coverslips within the same experiment. Analysis with MLM allows modelling of random intercepts and slopes of hierarchical data (Field, 2009), which would have allowed for statistical validation of this observation.

To meet the ANOVA assumption of even group sizes, data collection was terminated once 27 DRG images per condition were acquired. This led to data loss by necessity, despite meeting power requirements. Analysis with MLM would have accommodated for uneven group sizes (Field, 2009), allowed inclusion of the entire data set, and thus yielded a more representative data sample.

However, the current literature states that the minimum group size required to run MLM with 80% power is 1600 observations per condition (Brysbaert & Stevens, 2018), which equates to 3200 observations total for knockdown quantification. As it took me approximately an hour to acquire 20 cell images, it was determined that an MLM analysis requiring 160 hours of microscopy analysis alone was not realistically achievable within the scope of this project, despite its suitability to the data.

Knockdown has previously been calculated in the cellular neurobiology laboratory using three consecutive student's t tests (if normally distributed) or Mann-Whitney U tests (if not normally distributed) with alpha values for significance set at .05 (see Gasperini et al., 2009; Mitchell et al., 2012; Pavez et al., 2019)**.** However, an issue with running multiple tests with a *p* value of .05 is inflation of Type I error (Field, 2009). As such, the choice of a 3 x 2 ANOVA for analysis of somatic knockdown represents an improvement of standard protocols by reducing Type I error rate, and is a suitable compromise given the unattainable power requirements of MLM. Mann-Whitney U tests and *t* tests were only used in cases where the power requirements of ANOVA were not achieved.

Directions for Future Research

When grown on laminin, DRGs have bipolar morphology with identifiable axons and growth cones (Clark et al., 1993), and well-characterised responses to diverse chemoattractants (e.g., Gasperini et al., 2009; Gundersen & Barrett, 1989). However, this project failed to quantify Shank3 knockdown in DRG growth cones and was unable to measure corresponding effects on growth cone motility. Future projects may attain greater success studying Shank3 knockdown effects in cell types known to express Shank3 in the growth cone, such as cultured hippocampal cells (Naisbitt et al., 1999).

Glutaminergic NMDA and AMPA receptors mediate LTP in mature hippocampal cells (Siegelbaum & Kandel, 2013), a process disrupted by Shank3 knockout (Bozdagi et al., 2010). As Shank3 protein is present in hippocampal growth cones (Naisbitt et al., 1999), future research may seek to determine whether Shank3 knockdown disrupts glutamate-mediated axonal pathfinding in hippocampal cells via action on NMDA and AMPA receptors. This research would have strong

clinical significance, as abnormalities in hippocampal neural circuitry in embryo could potentially form the foundation for learning and memory difficulties seen in ID; a disorder often comorbid with ASD (American Psychological Association, 2013). Furthermore, the use of CNS-derived hippocampal cells (as opposed to PNS-derived DRGs) would increase generalisability of turning assay results to conclusions about brain development.

Investigating this research question would require development of a new dissection procedure for embryonic rat hippocampal cells. In order to isolate effects of Shank3 knockdown on NMDAR- and AMPAR-mediated glutaminergic signalling, it would be necessary to inhibit IP_3 signalling and resultant calcium release as a result of glutamate binding to mGluRs. This may be achieved by co-transfecting hippocampal cultures with siRNA for Shank3 and mGluR1/5, in order to knockdown expression of both proteins prior to completing glutamate-mediated turning assays.

Conclusion

The current study demonstrates localisation of pan-Shank protein in the growth cone of DRGs, and appears to demonstrate growth cone colocalization with Homer1b/c. These findings extend and enrich our understanding of peripheral neurodevelopment. Specifically, the results of this study build on findings by Miletic et al. (2010) and Han et al. (2016) showing Shank1 and Shank3 expression in mature DRGs, and suggest a role of pan-Shank protein in embryonic DRG circuitry.

This research project represents a step into exploring the role of Shank3 protein in guiding embryonic neurodevelopment. Whilst findings were limited due to cell culture and Shank3 knockdown issues, addressing these limitations in future

research is likely to yield novel results with clinical significance for understanding of ASD and neurodevelopmental disorders.

References

Alberts, B., Johnson, A., Lewis, J., Morgan, D., Raff, M., Roberts, K. & Walter, P. (2015). *Molecular Biology of the Cell*. New York: Taylor & Francis Group.

American Psychiatric Association (2013). Neurodevelopmental disorders. In *Diagnostic and Statistical Manual of Mental Disorders* (5th ed.). doi: 10.1176/appi.books.9780890425596.dsm.4

Ango, F., Pin, J. P., Tu, J. C., Xiao, B., Worley, P. F., Bockaert, J., & Fagni, L. (2000). Dendritic and Axonal Targeting of Type 5 Metabotropic Glutamate Receptor Is Regulated by Homer1 Proteins and Neuronal Excitation. *The Journal of Neuroscience, 20*(23), 8710. doi:10.1523/JNEUROSCI.20-23-08710.2000

Bailey, A., Le Couteur, A., Gottesman, I., Bolton, P., Simonoff, E., Yuzda, E. & Rutter, M. (1995). Autism as a strongly genetic disorder: Evidence from a British twin study. *Psychological Medicine*, *25*, 63-77. doi: 10.1017/s0033291700028099

Bargmann, C. I. & Gilliam, T. C. (2013). Genes and Behaviour. In E.R. Kandel., J. H. Schwartz., T. M. Jessell., S. A. Siegelbaum & A. J. Hudspeth (Eds.), *Principles of Neural Science* (pp. 39-65), US: McGraw Hill

Bashat, D. B., Kronfeld-Duenias, V., Zachor, D. A., Ekstein, P. M., Hendler, T., Tarrasch, R., . . . Sira, L. B. (2007). Accelerated maturation of white matter in young children with autism: A high b value DWI study. *Neuroimage, 37*(1), 40-47. doi: 10.1016/j.neuroimage.2007.04.060

Bozdagi, O., Sakurai, T., Papapetrou, D., Wang, X., Dickstein, D. L., Takahashi, N., . . . Buxbaum, J. D. (2010). Haploinsufficiency of the autism-associated

Shank3 gene leads to deficits in synaptic function, social interaction, and social communication. *Molecular Autism, 1*(1), 1-15. doi: 10.1186/2040-2392-1-15

Brakeman, P. R., Lanahan, A. A., O'Brien, R., Roche, K., Barnes, C. A., Huganir, R. L. & Worley, P. F. (1997). Homer: A protein that selectively binds metabotropic glutamate receptors. *Nature, 386*(20), 284-288. doi: 10.1038/386284a0

Brysbaert, M. & Stevens, M. (2018). Power analysis and effect size in mixed linear models: A tutorial. *Journal of Cognition, 1*(1), 1-20. doi:10.5334/joc.10

Clark, P., Britland, S. & Connolly, P. (1993). Growth cone guidance and neuron morphology on micropatterned laminin surfaces. *Journal of Cell Science, 105*, 203-212.

Costes, S. V., Daelemans, D., Cho, E. H., Dobbin, Z., Pavlakis, G. & Lockett, S. (2004). Automatic and quantitative measurement of protein-protein colocalisation in live cells. *Biophysical Journal, 86*, 3993-4003. doi: 10.1529/biophysj.103.038422

Courchesne, E., Carper, R. & Akshoomoff, N. (2003). Evidence of brain overgrowth in the first year of life in autism. *The Journal of the American Medical Association, 290*(3), 337-344. doi: 10.1001/jama.290.3.337

Du, Y., Weed, S. A., Xiong, W. C., Marshall, T. D. & Parsons, J. T. (1998). Identification of a novel cortactin SH3 domain-binding protein and its localisation to the growth cones of cultured neurons. *Molecular Cell Biology, 18*, 5838-5831.

Durand, C. M., Perroy, J., Loll, F., Perrais, D., Fagni, L., Bourgeron, T., . . . Sans, N. (2012). SHANK3 mutations identified in autism lead to modification of

dendritic spine morphology via an actin-dependent mechanism. *Molecular Psychiatry, 17*, 71. doi:10.1038/mp.2011.57

Elsabbagh, M., Divan, G., Koh, Y.-J., Kim, Y. S., Kauchali, S., Marcín, C. . . Fombonne, E. (2012). Global prevalence of autism and other pervasive developmental disorders. *Autism Research, 5*(3), 160-179. doi:10.1002/aur.239

Fan, J. & Raper, J. A. (1995). Localised collapsing cues can steer growth cones without inducing their full collapse. *Neuron, 14*, 263-274. Doi: 10.1016/0896-6273(95)90284-8

Field, A. (2009). *Discovering statistics using SPSS.* London: SAGE Publications Ltd

Gasperini, R., Choi-Lundberg, D., Thompson, M. J., Mitchell, C. B., & Foa, L. (2009). Homer regulates calcium signalling in growth cone turning. *Neural Development, 4*(1), 29. doi:10.1186/1749-8104-4-29

Gauthier, J. et al… (2010). De novo mutations in the gene encoding the synaptic scaffolding protein Shank3 in patients ascertained for schizophrenia. *Proceedings of the National Academy of Sciences in the United States of America, 107*(17), 7863-7868. doi: 10.1073/pnas.0906232107

Glazzard, J. & Overall, K. (2012). Living with autism spectrum disorder: Parental experiences of raising a child with autism spectrum disorder (ASD). *British Journal of Learning Support, 27*(1), 37-35. doi: 10.1111/j.1467-9604.2011.01505.x

Gundersen, R. W. & Barrett, J. N. (1980). Characterisation of the turning responses of dorsal root ganglia neurites toward nerve growth factor. *The Journal of Cell Biology, 87*, 546-554. doi: 10.1083/jcb.87.3.546

Halbedl, S., Schoen, M., Feiler, M. S., Boeckers, T. M. & Schmeisser, M. J. (2016). Shank3 is localised in axons and presynaptic specialisations of developing hippocampal neurons and involved in the modulation of NMDA receptor levels at axon terminals. *Journal of Neurochemistry*, *137*, 26-32. doi: 10.1111/jnc.13523

Hamdan, Fadi F., Gauthier, J., Araki, Y., Lin, D.-T., Yoshizawa, Y., Higashi, K., . . . Michaud, Jacques L. (2011). Excess of de novo deleterious mutations in genes associated with glutamatergic systems in nonsyndromic intellectual disability. *The American Journal of Human Genetics, 88*(3), 306-316. doi: 10.1016/j.ajhg.2011.02.001

Han, Q., Kim, Y. H., Wang, X., Liu, D., Zhang, Z. J., Bey, A. L., . . . Ji, R. R. (2016). Shank3 deficiency impairs heat hyperalgesia and TRPV1 signalling in primary sensory neurons. *Neuron, 92*(6), 1279-1293. doi: 10.1016/j.neuron.2016.11.007.

Hayashi, M. K., Tang, C., Verpelli, C., Narayanan, R., Stearns, M., Xu, R. M., . . . Hayashi, Y. (2009). The postsynaptic density proteins Homer and Shank form a polymeric network structure. *Cell*, *137*, 159-171. doi: 10.1016/j.cell.2009.01.050

Howlin, P., Goode, S., Hutton, J. & Rutter, M. (2004). Adult outcome for children with autism. *Journal of Child Psychology and Psychiatry*, *45*(2), 212-229. doi: 10.1111/j.1469-7610.2004.00215

Kater, S. B. & Mills, L. R. (1991). Regulation of growth cone behaviour by calcium. *The Journal of Neuroscience*, *11*(4), 891-899. doi: 10.1523/JNEUROSCI.11-04-00891.1991

Kaufman, L., Ayub, M., & Vincent, J. B. (2010). The genetic basis of non-syndromic intellectual disability: A review. *Journal of Neurodevelopmental Disorders, 2*(4), 182-209. doi:10.1007/s11689-010-9055-2

Leblond, C. S., Nava, C., Polge, A., Gauthier, J., Huguet, G., Lumbroso, S., . . . Bourgeron, T. (2014). Meta-analysis of SHANK Mutations in Autism Spectrum Disorders: a gradient of severity in cognitive impairments. *PLoS Genetics, 10*(9), e1004580. doi:10.1371/journal.pgen.1004580

Lin, C. H., & Forscher, P. (1993). Cytoskeletal remodeling during growth cone-target interactions. *The Journal of Cell Biology, 121*(6), 1369. doi:10.1083/jcb.121.6.1369

Marshall, C. R., Noor, A., Vincent, J. B., Lionel, A. C. Feuk, L., Skaug, J., . . . Scherer, S. W. (2008). Structural variation of chromosomes in Autism Spectrum Disorder. *The American Journal of Human Genetics, 82*, 477-488. doi: 10.1016/j.ajhg.2007.12.009

Miletic, G., Dumitrascu, C. I., Honstad, C. E., Micic, D. & Miletic, V. (2010). Loose ligation of the rat sciatic nerve elicits early accumulation of Shank1 protein in the post-synaptic density of spinal dorsal horn neurons. *Pain, 149*(1), 152-159. doi:10.1016/j.pain.2010.02.001

Mitchell, C. M., Gasperini, R. J., Small, D. H. & Foa, L. (2012). Stim1 is necessary for store-operated calcium entry in turning growth cones. *Journal of Neurochemistry, 122*, 1155-1166. doi: 10.1111/j.1471-4159.2012.07840.x

Monteiro, P., & Feng, G. (2017). SHANK proteins: roles at the synapse and in autism spectrum disorder. *Nat Rev Neurosci, 18*(3), 147-157. doi:10.1038/nrn.2016.183

Naisbitt, S., Kim, E., Tu, J. C., Xiao, B., Sala, C., Valtschanoff, J., . . . Sheng, M. (1999). Shank, a novel family of postsynaptic density proteins that binds to the NMDA receptor/PSD-95/GKAP complex and cortactin. *Neuron, 23*(3), 569-582. doi:10.1016/S0896-6273(00)80809-0

Pavez, M., Thompson, A. C., Arnott, H. J., Mitchell, C. B., D'Atri, I., Don, E. K., . . Foa, L. (2019). Stim1 is required for remodelling of the endoplasmic reticulum and microtubule cytoskeleton in steering growth cones. *The Journal of Neuroscience*, *26*, 5095-5114. doi: 10.1523/JNEUROSCI.2496-18.2019

Peça, J., Feliciano, C., Ting, J. T., Wang, W., Wells, M. F., Venkatraman, T. N., . . . Feng, G. (2011). Shank3 mutant mice display autistic-like behaviours and striatal dysfunction. *Nature, 472*(7344), 437-442. doi: 10.1038/nature09965

Phelan, K. & McDermid, H. E. (2011). The 22q13.3 deletion syndrome (Phelan-McDermid Syndrome). *Molecular Syndromology, 2*, 186-201. doi: 10.1159/000334260

Reichdart, L. F. (2006). Neurotrophin-regulated signalling pathways. *Philosophical Transactions of the Royal Society, 361*, 1545-1564. doi: 10.1098/rstb.2006.1894

Roussignol, G., Ango, F., Romorini, S., Tu, J. C., Sala, C., Worley, P. F., . . . Fagni, L. (2005). Shank expression is sufficient to induce functional dendritic spine synapses in aspiny neurons. *The Journal of Neuroscience*, *25*(14), 3560-3570. doi:

10.1523/JNEUROSCI.4354-04.2005

Sanes, J. R. & Jessell, T. M. (2013). The growth and guidance of axons. In E.R. Kandel., J. H. Schwartz., T. M. Jessell., S. A. Siegelbaum & A. J. Hudspeth (Eds.), *Principles of Neural Science* (pp. 1209-1232), US: McGraw Hill

Schmeisser, M. J., Ey, E., Wegener, S., Bockmann, J. A., Stempel, V., Kuebler, A., . . . Boeckers, T. M. (2012). Autistic like behaviours and hyperactivity in mice lacking ProSap1/Shank2. *Nature, 486*, 256-259. doi:10.1038/nature11015

Sheng, M. & Kim, E. (2000). The Shank family of scaffold proteins. *Journal of Cell Science, 113*, 1851-1856.

Siegelbaum, S. A. & Kandel, E. R. (2013). Prefrontal cortex, hippocampus, and the biology of explicit memory storage. In E.R. Kandel., J. H. Schwartz., T. M. Jessell., S. A. Siegelbaum & A. J. Hudspeth (Eds.), *Principles of Neural Science* (pp. 1487-1519), US: McGraw Hill

Sparks, B. F., Friedman, S. D., Shaw, D. W., Aylward, E. H., Echelard, D., Artru, A. A., . . . Dager, S. R. (2002). *Neurology*, *59*(2), 184-192. doi: 10.1212/WNL.59.2.184

Thermo Fisher Scientific. (2013). Silencer select pre-designed, validated and custom designed siRNA. Ambion by Life Technologies. Retrieved from: http://tools.thermofisher.com/content/sfs/manuals/Silencer_Select_PreDsignd_Vdtd_CustomDesign_siRNA_man.pdf

Tu, J. C., Xiao, B., Naisbitt, S., Yuan, J. P., Petralia, R. S., Brakeman, P., . . . Worley, P. F. (1999). Coupling of mGluR/Homer and PSD-95 complexes by the Shank family of postsynaptic density proteins. *Neuron, 23*(3), 583-592. doi:10.1016/S0896-6273(00)80810-7

Tu, J. C., Xiao, B., Yuan, J. P., Lanahan, A. A., Leoffert, K., Li, M., . . . Worley, P. F. (1998). Homer binds a novel proline-rich motif and links group 1 metabotropic glutamate receptors with IP3 receptors. *Neuron, 21*(4), 717-726. doi:10.1016/S0896-6273(00)80589-9

Wen, Z., Guirland, C., Ming, G. & Zheng, J. Q. (2004). A CaMKII/Calcineurin switch controls the direction of Ca^{2+} -dependent growth cone guidance. *Neuron*, *43*, 835-846. doi: 10.1016/j.neuron.2004.08.037

Wöhr, M., Roullet, F. I., Hung, A. Y., Sheng, M., & Crawley, J. N. (2011). Communication impairments in mice lacking Shank1: Reduced levels of ultrasonic vocalizations and scent marking behavior. *PLOS ONE*, *6*(6), e20631. doi:10.1371/journal.pone.0020631

Wu, S., Gan, G., Zhang, Z., Sun, J., Wang, Q., Gao, Z., . . . Zhang, Y. Q. (2017). A presynaptic function of Shank protein in drosophila. *The Journal of Neuroscience*, *37*(48), 11592-11604. doi: 10.1523/JNEUROSCI.0893-17.2017

Yoon, S.-Y., Kwon, S.-G., Kim, Y. H., Yeo, J.-H., Ko, H.-G., Roh, D.-H., . . . Oh, S. B. (2017). A critical role of spinal Shank2 proteins in NMDA-induced pain hypersensitivity. *Molecular Pain, 13*, 1744806916688902. doi:10.1177/1744806916688902

Yuan, J. P., Kiselyov, K., Shin, D. M., Chen, J., Shcheynikov, N., Kang, S. H., . . . Worley, P. F. (2003). Homer binds TRPC family channels and is required for gating of TRPC1 by IP_3 receptors. *Cell*, *114*, 777-789. doi: 10.1016/s0092-8674(03)00716-5

Zaslavsky, K., Zhang, W.-B., McCready, F. P., Rodrigues, D. C., Deneault, E., Loo, C., . . . Ellis, J. (2019). SHANK2 mutations associated with autism spectrum

disorder cause hyperconnectivity of human neurons. *Nature Neuroscience, 22*(4), 556-564. doi:10.1038/s41593-019-0365-8

Zheng, J. Q. & Poo, M. (2007). Calcium signalling in neuronal motility. *Annual Review of Cell and Developmental Biology*, *23*, 375-404. doi: 10.1146/annurev.cellbio.23.090506.123221

Zhou, Y., Sharma, J., Ke, Q., Landman, R., Yuan, J., Chen, H., . . Yang, S. (2019). Atypical behaviour and connectivity in Shank3-mutant macaques. *Nature*, *570*, 326-331. doi: 10.1038/s41586-019-1278-0